RBM10 Interacts with CTBNNBIP1 and Represses Lung Adenocarcinoma Progression Through the Wnt/β- catenin Pathway

Yingyue Cao
Harbin Medical University Third Clinical College: Tumor Hospital of Harbin Medical University
Xin Wang
Harbin Medical University Third Clinical College: Tumor Hospital of Harbin Medical University
Qingwei Meng
Harbin Medical University Third Clinical College: Tumor Hospital of Harbin Medical University
Jianxiong Geng
Harbin Medical University Third Clinical College: Tumor Hospital of Harbin Medical University
Shanqi Xu
Harbin Medical University Third Clinical College: Tumor Hospital of Harbin Medical University
Yaoguo Lang
Harbin Medical University Third Clinical College: Tumor Hospital of Harbin Medical University
Yongxu Zhou
Second Affiliated Hospital of Harbin Medical University
Lishuang Qi
Harbin Medical College: Harbin Medical University
Zijie Wang
Harbin Medical University Third Clinical College: Tumor Hospital of Harbin Medical University
Zixin Wei
Harbin Medical University Third Clinical College: Tumor Hospital of Harbin Medical University
Yan Yu (yuyan@hrbmu.edu.cn)
Harbin Medical University Third Clinical College: Tumor Hospital of Harbin Medical University
https://orcid.org/0000-0001-5598-763X
Bo Pan
Harbin Medical University Third Clinical College: Tumor Hospital of Harbin Medical University

Research

Keywords: RBM10, proliferation, metastasis, Wnt/β-catenin pathway, CTNNBIP1，lung adenocarcinoma

Posted Date: May 7th, 2021

DOI: https://doi.org/10.21203/rs.3.rs-480093/v1

Abstract

Background: RNA-binding motif protein 10 (RBM10), one of the RNA-binding protein (RBP) family, has a tumor suppressor role in various tumors. However, the functional role of RBM10 in lung adenocarcinoma (LUAD) and the molecular mechanism remain unclear. The aim of this study was to explore the effect of RBM10 on LUAD growth and metastasis and its molecular mechanism.

Methods: Bioinformatics analysis was used to predict RBM10 expression and its associations with clinicopathological features and prognosis in LUAD. Gain- and loss- of function experiments were conducted to investigate the biological functions of RBM10 both *in vitro* and *in vivo*. RNA-seq, bioinformatics programs, western blot, qRT-PCR, TOP/FOP flash reporter, co-immunoprecipitation (co-IP), nuclear and cytoplasmic protein extraction and rescue experiments were used to reveal the underlying mechanisms.

Results: Bioinformatics analysis showed that RBM10 was significantly downregulated and closely correlated with poor prognosis in LUAD patients. RBM10 silencing significantly promoted the LUAD proliferation, migration, invasion ability, while RBM10 overexpression had the opposite effects. Furthermore, upregulation of RBM10 inhibited growth and metastasis of LUAD *in vivo*. Additionally, RBM10 suppressed tumor progression through inhibiting epithelial to mesenchymal transition (EMT) in LUAD cells. Mechanistically, RBM10 interacts with β-catenin interacting protein 1 (CTNNBIP1) and positively regulates its expression, thus inactivating the Wnt/β-catenin pathway.

Conclusions: This is the first study that reported how RBM10 suppresses cell proliferation and metastasis of LUAD by negatively regulating the Wnt/β-catenin pathway through interaction with CTNNBIP1. These data suggest that RBM10 may be a promising new target or clinical biomarker for LUAD therapy.

Background

Lung cancer remains the most common malignancy associated with high morbidity and mortality [1]. In 2020, 2.2 million new cases (11.4%) and 1.8 million deaths (18%) occurred worldwide [2]. Lung adenocarcinoma (LUAD) represents the most frequent histological type of lung cancer [3]. Targeted therapies, including epidermal growth factor receptor (EGFR) mutations, anaplastic lymphoma kinase (ALK) translocation, and ROS proto-oncogene1 (ROS1) fusion [4–6], have shown to be effective in patients with lung cancer. Although these therapies have improved progression-free survival and overall survival in patients with lung cancer, the 5-year survival rate for LUAD patients remain lower than 15% [7], mainly because the specificity and applicability of targeted drugs is limited. Thus, uncovering the molecular mechanisms involved in LUAD progression and identifying new therapeutic targets for LUAD is of crucial importance.

RBM10, also known as S1–1, is often deleted or mutated in malignant cells [8–11], including lung adenocarcinoma (LUAD)[9, 12]. The major biological functions of RBM10 include regulation of mRNA stabilization, alternative splicing, nuclear output, and translation [13–15]; yet, the exact role of RBM10 in

cancer progression remains controversial. Loss of RBM10 can promote cell proliferation, migration, and invasion in osteosarcoma [16]. Furthermore, RBM10 can promote the BAX expression in breast cancer, which suggests that RBM10 is a potential tumor suppressor [17]. However, other studies suggested that RBM10 might have a pro-cancer role as a tumor promoter or a pro-oncogene [13, 18–20]. In invasive melanoma, higher RBM10 expression was positively correlated with increased disease aggression [21]. RBM10 expression contributes to tumor growth and metastasis in RBM5-null tumors [18]. In our previous study, we performed second-generation sequencing of samples collected from 19 patients with LUAD with metastasis and found that RBM10 was downregulated in LUAD. Moreover, low expression of RBM10 was associated with late clinical stage and poor prognosis of lung adenocarcinoma patients. Therefore, we hypothesized that RBM10, as a tumor suppressor gene, may be involved in lung adenocarcinoma progression.

Epithelial-mesenchymal transition (EMT) is considered a key indicator in the initial step of cancer metastasis [22, 23]. EMT is a complex process that involves multiple signaling pathways, including the Wnt/β-catenin signaling pathway, PI3K/AKT signaling pathway, TGF-β signaling pathway, and MAPK signaling pathway [24]. A Wnt/β-catenin signaling pathway is one of the most important signaling pathways, whose dysregulation is often seen in malignant cells, including LUAD [25–27]. The Wnt/β-catenin pathway is an important regulator of EMT; its activation facilitates EMT to promote invasion and metastasis of various tumors [28, 29]. CTNNBIP1 (also known as ICAT), is one of the β-catenin negative regulatory factors, which binds to β-catenin and prevents the interaction between β-catenin and the TCF/LEF complex. This inactivates the transcription of target genes downstream of the Wnt pathway, thereby inhibiting the activation of the Wnt/β-catenin signaling pathway [30]. Therefore, it is often used as an inhibitor of the Wnt/β-catenin pathway. Previous studies have reported that CTNNBIP1 is involved in the progression of various tumors, including malignant melanoma [31], glioblastoma [32], colorectal cancer [33], and cervical cancer [34]. In lung cancer, ectopic expression of CTNNBIP1 can inhibit cell migration, while its down-regulation can cause an opposite effect [35]. However, so far, no study has reported on the relationship between RBM10 and CTNNBIP1 in LUAD.

The aim of this study was to determine whether RBM10 could suppress LUAD progress and metastasis by regulating EMT via the Wnt/β-catenin signaling pathway.

Materials And Methods

Bioinformatics analysis

The Oncomine (http://www.oncomine.org), GEPIA (http://gepia.cancer-pku.cn/) and UALCAN (http://ualcan.path.uab.edu) were used to analyze the mRNA expression level of RBM10 or CTNNBIP1 in LUAD tissues and the normal lung tissues. The Kaplan - Meier plotter (http://kmplot.com) database was used to analyze the correlation between RBM10 expression and survival prognosis in patients with LUAD.

Fresh human LUAD tissue collection

Six paired fresh samples, including LUAD tumor and adjacent normal lung tissues, were collected from the Third Clinical Thoracic Surgery Department, Harbin Medical University, according to clear pathological diagnosis and patient informed consent. All procedures were approved by the Third Clinical Ethics Committee of Harbin Medical University.

Cell culture

Human LUAD cell lines H1299, H1915, H1650, A549, H1975, H661, H827, and PC-9, and the normal lung epithelial cell line HBE were all obtained from American Type Culture Collection (ATCC). All culture media were supplemented with 10% fetal bovine serum (FBS, PAN, Biotech GmbH, Germany). PC-9 was cultured in Dulbecco's Modified Eagle's Medium (DMEM, Gibco®, Grand Island, NY, USA), while the remaining cell lines were cultured in RPMI-1640 (Gibco®) at 37°C in a humidified atmosphere containing 5% CO2. Cells used in experiments were in good condition without mycoplasma contamination.

Cell Transfection

The small-interfering RNA (siRNA) targeting RBM10 and CTNNBIP1 were purchased from Ribobio (Guangzhou, China). The used siRNA sequences were: RBM10 siRNA-1, GCATGACTATGACGACTCA; RBM10 siRNA-3, CGACGGACATAAGGAGACA, and CTNNBIP1, siRNA-1, 5'-GAUGGGAUCAAACCUGACA-3'. A negative siRNA control (si-NC) with the sequence 5'-UUCUCCGAACGUGUCACGUTT-3' was also used.

A549 and H1299 cell lines were cultured on a 6-well plate for 24h. Cells were then using 10μl of the required siRNA (50μM) together with 10μl jet-PRIME (Poly-plus Transfection, France) according to the manufacturer's instructions. The design of the overexpression RBM10 sequence and the packaging of lentiviruses were completed by the Han bio Biotechnology Company (Shanghai, China). A549 and H1299 cell lines were infected with lentivirus using polybrene (6μg/ml) and then selected with puromycin (2μg/ml) for 14 days to establish the stable RBM10-overexpressing cell lines. The transfection efficiencies were verified by qRT-PCR and western blot.

Quantitative real-time PCR (qRT-qPCR) analysis

Total RNA was isolated from LUAD cells or fresh tumor tissues using TRIzol reagent (Invitrogen, Carlsbad, CA, USA) according to the manufacturer's instructions. The cDNA was obtained through reverse transcription with a Fast Quant RT Kit (TIANGEN, China). GAPDH was used as the internal control. qRT-PCR was conducted on a 7500 fast PCR System (Applied Biosystems, Foster City, CA, USA) using Talent qPCR Pre-Mix (SYBR Green; TIANGEN, China). The specific mRNA expression level was quantified using the $2 - \Delta\Delta CT$ method. The primers utilized in qRT-PCR are listed in **Additional file 1: Table S1**.

Western blot

The standard Western blot experiment was performed as previously described [36], using 60μg protein samples from fresh tissues and cells. The antibodies used for the Western blot analysis are listed in **Additional file 2: Table S2**. Each experiment was run in triplicate,

Cell proliferation assays

Cells were counted and seeded in 96-well plates (5×10^3 cells/well). After incubation for 24h, 10μl of Cell Counting Kit-8 (CCK-8, Dojindo, Kumamoto, Japan) was added to the culture medium and incubated for 1.5h at 37°C. Then, the optical density (OD) value at 450nm was measured. Three independent experiments were performed.

Clone formation assay

Transfected cells (700 cells/well) were counted and plated in 6-well plates. After 14 days of culture, cells were fixed with 0.4% paraformaldehyde for 15min and were then stained with 0.5% crystal violet for 30min. Colonies containing more than 50 cells were counted. Three independent experiments were performed.

5-Ethynyl-2'-deoxyuridine (EdU) incorporation assay

After transfection, the LUAD cells were inoculated into 24-well plates. EdU kit (RiboBio, Guangzhou, China) was used for labeling cells following the manufacturer's instructions. Photographs were taken using an inverted fluorescent microscope (Leica Microsystems Inc., USA), and the experiment was repeated three times.

Soft agar colony formation assay

Soft agar colony formation assay (GENMED SCIENTIFICS INC, USA) was performed according to manufacturer's instructions. Briefly, 1.5mL GENMED Cloning Solution (Reagent A) and 1.5mL GENMED Hypertrophic Solution (Reagent B) were mixed and added into the 12-well plate, after which the substrate was solidified. Next, 1ml GENMED aqueous reagent (Reagent C) with 500ul GENMED clonal reagent (Reagent A) and 200μl cell suspension (containing 2500 cells) were mixed and immediately added into the 12-well plate. The colloid was set at room temperature for 2h and incubated overnight at 37℃ and 5% CO_2. The next day, 1mL GENMED Reagent D was added into the 12-well plate and cultured at 37℃ and 5% CO_2 for 4 weeks. Photographs were taken under an inverted microscope (Leica Microsystems Inc., USA). Three independent experiments were performed.

Wound healing assay

After transfection, the A549 and H1299 cells were seeded into 6-well plates. When the cell density reached over 80%, a 200μl pipette tip was used to scratch three separate wounds through the cells, moving perpendicular to the line. The cells were then gently rinsed twice with PBS to remove floating cells and cultured in the medium containing 0.5% FBS serum for 48 hours. Images of the scratches were taken using an inverted microscope (Olympus, Tokyo, Japan) at ×10 magnification at 0 and 48 h of incubation. The experiments were run in triplicate.

Transwell assay

In brief, 3 ~ 5×10^5 cells were resuspended in 300ul serum-free medium and then seeded in the upper chamber (BD Biosciences, New Jersey, USA) pre-coated with or without 40μl diluted Matrigel, while 700μl medium supplemented with 10% FBS was added in the lower chamber. After 24h or 48h, cells on the top

surface of the microporous membrane were wiped off with a cotton swab. The remaining cells were fixed with 4% paraformaldehyde, stained with 0.1% crystal violet, and counted under a microscope (Leica Microsystems Inc., USA). The experiments were repeated three times.

FITC-phalloidine cytoskeleton staining and cell immunofluorescence staining

Cells were slightly washed by preheated (37°C) PBS 3 times and fixed in 4% paraformaldehyde for 20 min. Then, the cells were permeated with 0.5% Triton X-100 for 5 min and blocked in 5% BSA for 1h at room temperature. For FITC-phalloidine cytoskeleton staining, F-actin was stained with TRITC (SolarBio, Beijing, China) containing 1% BSA for 40 min at room temperature. For cell IF staining, the cells were incubated with the rabbit polyclonal anti-E-cadherin antibody (diluted 1:100) and the rabbit polyclonal anti-Vimentin antibody (diluted 1:100) primary antibodies at 4°C overnight. The next day, the relevant secondary antibodies were added to the above cells for 1h at room temperature. The nuclei were stained with DAPI for 5 ~ 8min. The cells were imaged using an inverted fluorescence microscope (Leica Microsystems Inc., USA).

TOP/FOP flash reporter assay

A549 and H1299 with stable RBM10 overexpression were cultured in 24-well plates (2×10^4 cells per well). After 24h, cells were transfected with the TOP-Flash or FOP-Flash reporter plasmids together with pRL-TK using Lipofectamine 2000 (Invitrogen). After 48h of culture, the luciferase activity was analyzed using a dual-luciferase reporter kit (Promega). Data are presented as the ratio of relative light units of TOP flash to FOP flash from triplicate experiments.

Nuclear and cytoplasmic protein extraction

Cytosolic and nuclear protein extraction was performed using a Minute™ Cytoplasmic and Nuclear Extraction Kit for Cells (Invent, SC-003) according to the manufacturer's instructions. In brief, the cells were washed twice with cold PBS, after which the buffer was completely aspirated. Cells were then mixed with an appropriate amount of cytoplasmic extraction buffer and placed on ice for 5min, centrifuged for 5min at 14,000×g at 4°C, after which the supernatant was collected (cytosol fraction). Next, samples were mixed with an appropriate amount of nuclear extraction buffer to pellet, vigorously vortexing for 60 seconds, and then incubated on ice for 15min; this procedure was repeated 4 times, after which samples were centrifuged for 2min at 14,000×g. Each fraction was tested for the presence of the cytosolic marker β-actin and the nuclear marker laminB1 by Western blotting as appropriate. Each experiment was performed three times.

Co-immunoprecipitation (Co-IP)

Co-immunoprecipitation was conducted according to manufacturer's operations (Absin Bioscience *Inc*, china). Briefly, the cells were washed three times with ice-cold PBS. The cell lysate was then collected at 4°C using immunoprecipitation lysis buffer supplemented with protease inhibitor (Roche, Basel, Switzerland). The 500μl of cell lysates (containing total protein 200-1000ug) were precleared with 5μl of

protein A and protein G agarose beads at 4℃ for 2h. Then, the cell lysates (500μL) were incubated with 5μg of the antibody and 1ug of the normal IgG antibody at 4°C overnight. The next day, samples were mixed with an immunoprecipitation mixture (5μl of protein A and protein G beads) for 3h. The immune-complex was collected, washed 6 times with cold IP buffer by a 2min centrifugation at 12,000×*g.* Samples were analyzed by Western blotting. Each experiment was performed three times.

Chemicals

XAV-939 (a specific inhibitor of Wnt/β-catenin signaling) and CHIR-99021 (a specific activator of Wnt/β-catenin signaling) were purchased from Selleckchem. All agents were used according to the manufacturers' instructions.

Animal experiments

Female nude mice (BALB/c, 4 weeks) were purchased from Beijing Vital Li Hua Experimental Animal Technology Company (Beijing, China). Animals were raised in pathogen-free conditions with a temperature of 22 ± 1 ºC, relative humidity of 50 ± 1%, and a light/dark cycle of 12/12 hr. All animal studies (including the mice euthanasia procedure) were done in compliance with the regulations and guidelines of Harbin Medical University institutional animal care and conducted according to the AAALAC and the IACUC guidelines.

For xenograft model construction, 2.5 × 10^7/150μl A549 cells with or without stable RBM10 overexpression were subcutaneously injected into 4 weeks BALB**/**c nude mice (n = 5 mice per group). The length and width of tumors were measured every 4 days with a caliper, and the tumor volume (mm^3) was calculated with the formula: tumor volume (mm^3) = 0.5 × (length × width)^2. The progression of xenograft growth was analyzed on day 32 using *in vivo* imaging system, after which the mice were sacrificed, the tumor dissected, weighed, and fixed in formalin.

For lung metastasis models, the same female nude mice were injected with 1 × 10^7/150μl A549 cells with or without stable RBM10 overexpression via the tail vein. The mice were sacrificed after seven weeks, after which the lungs were excised and then analyzed in *ex vivo* using bioluminescence imaging (BLI) and hematoxylin and eosin (H&E) staining.

IHC and H&E staining

IHC was performed as previously described [36]. For primary antibody incubation, ki67 (27309-1-AP, Proteintech, 1:100), E-cadherin (20874-1-AP, Proteintech, 1:1000), Vimentin (10366-1-AP, Proteintech, 1:1000), c-MYC (CY5150, Abways, 1:40) and cyclinD1 (CY5404, Abways, 1:40) were used for IHC. For H&E staining, after dewaxing and rehydrating, longitudinal sections of 5μm were stained with hematoxylin solution for 5min, then soaked in 1% acidic ethanol (1% HCl in 70% ethanol) for 5 times, and finally rinsed in distilled water. The sections were then stained in eosin solution for 3min, then dehydrated with gradient alcohol, and clarified in xylene. Eventually, a microscope (Olympus, Toyo, Japan) was used to observe the tissue sections.

Statistical analysis

Statistical analysis was performed with GraphPad Prism 6.0 software (San Diego, California, USA). All data were shown as the mean ± SD, unless declared. Data were analyzed using Student's t-test for two groups or one-way analysis of variance (ANOVA) for three or more groups. A *P* value < 0.05 was considered to be statistically significant.

Results

Low RBM10 expression is associated with a poor prognosis in LUAD

Based on Bhattacharjee lung statistics from Oncomine database (http://www.oncomine.org), the mRNA expression of RBM10 was significantly downregulated in LUAD tissues compared with corresponding normal lung tissues ($p < 0.05$, Fig. 1a). The RBM10 expression gradually decreased with clinical stage progression from TCGA and GTEx database in GEPIA website (http://gepia.cancer-pku.cn/) (Fig. 1b **~ c**). Moreover, Western blot analysis showed that RBM10 protein expression was significantly downregulated in LUAD fresh tissues (Fig. 1d). Consistently, the results of qRT-PCR analysis also showed that RBM10 mRNA expression was lower in LUAD cell lines (H1299, H1915, H1650, A549, H1975, H661, H827, PC-9) compared with the normal lung epithelial cell line HBE (Fig. 1e). In addition, the Kaplan–Meier plotter database (http://kmplot.com) analysis showed that patients with low RBM10 expression levels had poor overall survival (OS) compared to patients with high RBM10 expression levels (HR = 0.72, Log-rank P = 0.0068, Fig. 1f). Taken together, these results indicated that expression of RBM10 is low and is positively associated with poor prognosis in LUAD patients.

RBM10 inhibits cell proliferation, migration, and invasion of LUAD cells in vitro

The above data showed that A549 and H1299 cells have a moderate RBM10 expression level (Fig. 1e). Next, in one group, we silenced RBM10 in those cells with RBM10-siRNA to knock down RBM10 expression; in the other cell group, RBM10 was stably overexpressed using an RBM10 lentivirus. Both the overexpression and knockdown efficiencies of RBM10 were confirmed by qRT-PCR and Western blot assays (**Additional file 1: Figure S1**). We then performed a variety of *in vitro* experiments to evaluate the effect of RBM10 expression on cell proliferation, migration, and invasion of LUAD cells. The CCK-8 and EdU assays showed that RBM10 knockdown significantly increased cell viability and enhanced the DNA synthesis ability of both A549 and H1299 cells (Fig. 2a, c, e), while forced RBM10 expression caused an opposite effect (Fig. 2b, d, e). Moreover, the inhibition of RBM10 led to the generation of more and larger cell colonies compared with the control groups, while overexpressing RBM10 reduced both colony size and number in the A549 and H1299 cells (Fig. 2f **~ h**). These findings were further confirmed in soft agar colony formation assays (**Additional file 1: Figure S2**). We also found that RBM10 silencing promoted the invasion and migration ability of A529 and H1299 cells, whereas RBM10-overexpressing LUAD cells

reduced the cell invasion and migration capacity (Fig. 2i **~ t**). Thus, this data suggests that RBM10 may inhibit tumor cell proliferation, migration, and invasion of LUAD cells *in vitro*.

RBM10 suppresses LUAD cell tumorigenesis and metastasis in vivo

Next, we explored that RBM10 suppressed LUAD tumorigenesis and metastasis *in vivo*. A xenograft tumor mouse model was established by subcutaneously injecting 2.5×10^7/150μl A549-Vector and A549-RBM10 cells into the left armpit of 4 weeks BALB**/**c nude mice (**Additional file 2: Figure S1a**). Western blot assay showed that RBM10 was stably overexpressed in A549 cell lines (**Additional file 2: Figure S1b**). As shown in Fig. 3a and 3b, tumor volumes significantly decreased in the A549-RBM10 group compared with the A549-vector group. At the end of the experiments, the mice were sacrificed, the subcutaneous tumors were isolated, and their volume and weights were measured. The results showed that tumor volume was markedly decreased in the A549-RBM10 group when compared with the A549-Vector group (Fig. 3c, d, $P < 0.05$). Furthermore, IHC analyses showed that the xenograft tumors from the A549-RBM10 group displayed a lower level of Ki67 relative to control (A549-Vector) (Fig. 3e).

We also used the tail vein injection mouse model to investigate the influence of RBM10 in LUAD metastasis *in vivo* (**Additional file 2: Figure S2**). On day 49 after inoculation, the mice were sacrificed, the lungs were collected, and metastatic nodules were counted. The results indicated that the number and the size of lung metastasis lesions were significantly decreased in mice injected with A549-RBM10 cells relative to control (A549-Vector) cells (Fig. 4a **~ c**). Moreover, fewer mice in the A549-RBM10 group (1/5, 20%) showed lung metastasis, while in the control group (A549-Vector), all mice developed lung metastasis (4/5, 80%, Fig. 4d). In addition, we also found that the A549-RBM10 group had smaller and fewer lung metastatic foci than those in the control group (A549-vector) (Fig. 4e). Collectively, these data indicated that RBM10 overexpression inhibited LUAD lung metastasis *in vivo*.

RBM10 inhibits the EMT program of LUAD

Current evidence suggests that epithelial-mesenchymal transition (EMT) is a key step in the progression of cancer metastasis [22]. Through mRNA expression correlation analysis on the TCGA database, we found that the expression of RBM10 is positively correlated with CHD1 (also called E-cadherin) but negatively correlated with Vimentin (VIM), ZEB1, and ZEB2 (Fig. 5a and **Additional file 3: Figure S1**), thus indicating that RBM10 might participate in EMT process of LUAD. The cytoskeleton can trigger microfilament structural changes and increase the number of pseudopodia (lamellipodia and filopodia), which is responsible for cancer cells' invasive and migratory properties [37]. FITC-phalloidine cytoskeleton staining was performed to evaluate morphological alterations in LUAD cells. The results showed that RBM10-silencing cells formed a large number of visible actin filaments and pseudopodia compared with control cells, while RBM10-overexpressing cells had clear and round cell shapes bearing scarcely actin remodeling (Fig. 5b, c).

Next, we evaluated whether EMT markers were altered. Using immunofluorescence (IF) assays, we observed that the fluorescence intensity of E-cadherin decreased and Vimentin increased in the RBM10 silencing cells, whereas RBM10 overexpression upregulated E-cadherin fluorescence but downregulated Vimentin (Fig. 5d **~ g**). A similar result was also revealed by IHC in tumor tissues from xenograft tumors (**Additional file 3: Figure S2**). Western blot analysis demonstrated that RBM10 silencing increased Vimentin, N-cadherin, slug, and twist protein expression levels, whereas E-cadherin and EPCAM protein expression levels were decreased in A549 and H1299 cells (Fig. 5h, i). Conversely, overexpression of RBM10 showed the opposite effect (Fig. 5j, k). Additionally, we also evaluated the mRNA expression of E-cadherin, Vimentin, slug, and twist in LUAD cells, and changes of mRNA expression were consistent with that observed at the protein level (**Additional file 3: Figure S3**). Furthermore, qRT-PCR assays showed that downregulation of RBM10 clearly increased the mRNA levels of ZEB1, ZEB2, MMP3, MMP7, and MMP10, while upregulation of RBM10 markedly reduced their mRNA expression (**Additional file 3: Figure S4**). Thus, these results strongly suggested that RBM10 inhibited EMT.

RBM10 negatively regulates the Wnt/β-catenin signaling pathway

To elucidate the underlying molecular mechanisms through which RBM10 regulates LUAD progression, the RNA sequencing (RNA-seq) was performed using H1299 cells that express either control si-NC or si-RBM10. Gene ontology (GO) enrichment analysis revealed that RBM10-dependent genes were involved in either biological processes such as biological adhesion, cell proliferation, and growth, or cellular component, including cell junction (**Additional file 4: Figure S1a**), supporting a role for RBM10 in cell proliferation and EMT. KEGG pathway analysis showed that these genes were significantly associated with cancer-related functions, including cellular motility, growth and death and etc. (**Additional file 4: Figure S1b**). More importantly, pathway enrichment analysis suggested that multiple signaling pathways might participate in the tumor-promoting mechanism of silencing RBM10, such as the Wnt**/**β-catenin signaling pathway, NF-KB signaling pathway, TGF-β signaling pathway (**Additional file 4: Figure S2**). Based on ChipBase and StarBase databases, we found that the expression of RBM10 was markedly negatively correlated with the four common Wnt**/**β-catenin signaling pathway target genes such as CTNNB1(also called β-catenin), Wnt5a, c-MYC, and CD44 in LUAD (**Additional file 4: Figure S3**). Hence, Wnt/β–catenin signaling was selected for further research.

We performed TOP**/**FOP flash luciferase reporter assays. The results showed that RBM10 overexpression significantly reduced the activity of the TOP**/**FOP-flash reporter genes in both A549 and H1299 cells compared to control cells (Fig. 6a), thus suggesting that RBM10 inhibits the WNT**/**β-catenin signaling activity in LUAD cells. Interestingly, qRT-PCR and Western blot indicated that RBM10 knockdown significantly increased the expression of endogenous β-catenin in LUAD cells (Fig. 6b, c, **Additional file 4: Figure S4a, b**), while overexpression of RBM10 markedly reduced the expression of β-catenin (Fig. 6d, e, **Additional file 4: Figure S4c, d**). Furthermore, we performed the nuclear and cytoplasmic cellular fractions. Western blot assays results showed that the level of β-catenin in the nucleus was increased, while that in

the cytoplasm was decreased by silencing RBM10 (Fig. 6f, g). In contrast, overexpressing RBM10 made impaired nuclear β-catenin and induced cytoplasmic β-catenin (Fig. 6h, i).

Moreover, the subcellular localization of β-catenin in A549 cells detected by immunofluorescence (IF) analysis further supported our hypothesis. The results indicated that downregulation of RBM10 increased the concentration of β-catenin in nuclear and blocked the β-catenin in the cytoplasm in A549 cells (Fig. 6j), while upregulation of RBM10 decreased the expression of β-catenin in nuclear and enhanced the β-catenin in the cytoplasm (**Additional file 4: Figure S5**).

We also examined the expression of c-MYC, cyclin D1, and MMP7, which are important downstream target genes of the Wnt/β-catenin signaling pathway [38, 39]. As shown in Fig. 6b **~ e** and **Additional file 4: Figure S4a ~ d**, the results indicated that the mRNA and protein expression levels of c-MYC, MMP7, and cyclinD1 were up- or down-regulated when RBM10 was silenced or overexpressed in A549 and H1299 cells. In addition, IHC staining showed that c-MYC and cyclinD1 expression was lower in xenograft tumors with RBM10 overexpression (**Additional file 4: Figure S6**).

To further investigate the functions of Wnt/β-catenin signaling on the progression of LUAD, cells were treated with Wnt/β-catenin pathway activator CHIR 99021 [40] or inhibitor XAV93 [41]. As shown in Fig. 6k, l, when cells were treated with XAV-939 (10μl) for 24h, Transwell assays indicated that the migration and invasion ability of A549 and H1299 RBM10 silencing cells was significantly decreased. However, CHIR 99021 promoted the migration and invasion ability of RBM10-overexpressing cells (Fig. 6m, n). Furthermore, Western blot showed that CHIR 99021 reverses the effect of RBM10 overexpressed on EMT markers (E-cadherin and twist) expression (Fig. 6o). Altogether, all these data indicated that depletion of RBM10 might promote LUAD cell proliferation and metastasis through promoting the activation of the Wnt/β-catenin pathway.

RBM10 interacts with CTNNBIP1

TCGA analysis showed that mRNA expression of CTNNBIP1 was markedly lower in most solid cancer tissues, including in LUAD (**Additional file 5: Figure S1a**). UALCAN (http://ualcan.path.uab.edu/index.html) and StarBase analysis showed that RBM10 expression was significantly downregulated in LUAD compared to that of normal lung tissues (**Additional file 5: Figure S1b, c**). GEPIA website indicated that the mRNA expression of CTNNBIP1 was decreased in lung adenocarcinoma tissues and negatively corrected with clinical stage of lung adenocarcinoma patients, which was similar to the expression pattern of RBM10 (**Additional file 5: Figure S1d, e**). Furthermore, qRT-PCR assays showed that the CTNNBIP1 mRNA expression was low in LUAD cell lines (**Additional file 5: Figure S1f**). Kaplan-Meier survival curves revealed that low CTNNBIP1 expression in LUAD correlated with poor survival (HR = 0.67, Log-rank P = 0.012, **Additional file 5: Figure S1g**). These results suggested that CTNNBIP1 has low expression in lung adenocarcinoma and that it has a tumor-suppressive role.

We further analyzed the expression pattern of RBM10 and CTNNBIP1 in Landi lung statistics from the Oncomine database. The results showed that CTNNBIP1 exhibited a similar expression pattern with

RBM10, both of which had low expression in LUAD tissues (Fig. 7a, b). In addition, the correlation between RBM10 and CTNNBIP1 was analyzed using the LUAD-TCGA data collection from the StarBase database; the results showed that RBM10 expression was positively correlated with CTNNBIP1 (Fig. 7c). Based on these data, we inferred that RBM10 interacts with CTNNBIP1, which was then confirmed by the co-IP assay (Fig. 7d, e); co-IP assay of the nuclear and cytoplasmic cellular fractions showed that RBM10 mainly interacted with CTNNBIP1 in the nucleus (Fig. 7f).

For further exploration of the regulatory relationship between RBM10 and CTNNBIP1, we used Western blot and qRT-PCR assays to detect their expressions. As shown in Fig. 7g, h, RBM10 silencing decreased the CTNNBIP1 protein level in A549 and H1299 cells, while RBM10-overexpression caused an opposite effect. In addition, down-regulation or upregulation of RBM10 did not significantly alter the levels of CTNNBIP1 mRNA transcripts in A549 and H1299 cells (Fig. 7i). These findings suggested that CTNNBIP1 might be downstream of RBM10. RBM10 positively regulates CTNNBIP1, and its expression is regulated by RBM10 at the protein levels.

In line with these results, we also conducted rescue experiments. In A549 and H1299 cells with stable overexpression of RBM10, si-CTNNBIP1 was transiently transfected to down-regulate the expression of CTNNBIP1. Using wound healing assay and Transwell assay, we observed that RBM10 significantly reduced cell invasion and migration in A549 and H1299 cells while silencing CTNNBIP1 reversed this process (**Additional file 5: Figure S2**). Collectively, these data demonstrate that RBM10 interacts with CTNNBIP1 and reduces the protein expression of CTNNBIP1 in LUAD.

RBM10 inhibits the Wnt/β-catenin pathway by blocking the β-catenin-TCF/LEF interaction

The precise molecular mechanisms through which RBM10 suppresses the Wnt/β-catenin pathway activity in LUAD cells were further elucidated. CTNNBIP1, as an inhibitor of β-catenin, can directly bind with β-catenin and impair the interaction between β-catenin and TCF/LEF complex, and subsequently inhibits Wnt/β-catenin signaling pathway. StarBase database showed that the mRNA expression of RBM10 was positively correlated with the expression of CTNNBIP1 (Fig. 7c) but negatively corrected with the expression of TCF4 and LEF1 (Fig. 8a, b). Upregulation of RBM10 led to low expression levels of TCF3, TCF4, and LEF1 (Fig. 8c **~ f**). Therefore, we performed co-IP assays to further confirm whether RBM10 regulated the Wnt/β-catenin pathway through CTNNBIP1. As shown in Fig. 8g **and h**, we observed that RBM10 overexpression markedly inhibited the association of β-catenin with TCF/LEF while enhancing the interaction between β-catenin and CTNNBIP1. In general, these results proved that RBM10 inactivated the Wnt/β-catenin pathway by increasing the inhibitory role of CTNNBIP1 and blocking the β-catenin-TCF/LEF interaction.

Discussion

Our previous study indicated a high frameshift mutation of RBM10 in LUAD (2/19, approximately 10.5%), which was distributed throughout the coding region rather than at specific sites; this data are similar to

the classical tumor suppressor gene mutation spectrum (article to be published)[42]. Previous studies have confirmed that frameshift mutations usually decrease or lose the gene's function. In this research, bioinformatics analysis showed that RBM10 was down-regulated in LUAD tissues compared with normal lung tissues, and the expression of RBM10 gradually decreased with the progression of clinical stages. Kaplan-Meier analysis results showed that low RBM10 expression had a significantly shorter survival time and poor prognosis, thus suggesting that the low RBM10 expression was a marker of poor prognosis in LUAD. Based on this, we speculated that RBM10 is involved in LUAD progression as a tumor suppressor gene.

To date, only a few studies have shown that RBM10 is involved in tumor metastasis [18, 21]. Garrisi *et al* [21] reported that high RBM10 expression was correlated with increased disease aggression in melanoma cancer. Furthermore, Julie *et al* [43] found that RBM10 promotes transformation-associated processes in RBM5-null SCLC cells. However, so far, there are no studies on the involvement of RBM10 in metastasis and progression of lung adenocarcinoma. Our study revealed that RBM10 knockdown markedly promoted the proliferation, migration, and invasion ability of LUAD cells, while RBM10 overexpression had the opposite effects. We further confirmed the inhibiting effect of RBM10 on tumor growth and lung metastasis of LUAD *in vivo.* Together, our studies clearly indicate that RBM10 inhibited proliferation and metastasis of LUAD cells by regulating EMT.

Next, we explored the underlying mechanism of RBM10 inhibiting the process of LUAD. Firstly, using RNA-seq and KEGG pathway enrichment analysis, we found that RBM10 is involved in a variety of signaling pathways, including the Wnt signaling pathway, NF-kB signaling pathway, and TGF-β signaling pathway. Aberrant activation of the Wnt/β-catenin pathway can promote EMT, invasion, and metastasis of various cancers [44]. Wnt/β-catenin pathway activation has been reported in around 50% of human NSCLC cell lines [45]. RBM10 and RBM5 have 50% amino acid homology and share functional similarities [46, 47]. It has been suggested that RBM5 functions as an anticancer by inhibiting the Wnt/β-catenin pathway [48, 49]. Therefore, we herein detected if RBM10 inhibited LUAD progress by regulating the Wnt/β-catenin signaling pathway.

Combined with TGCA databases, we found that RBM10 expression was negatively regulated with Wnt/β-catenin pathway target genes (CTNNB1, c-MYC, MMP7, CD44). The TOP/FOP, luciferase activity assay showed the Wnt/β-catenin signaling activity was attenuated by RBM10 overexpression. Additionally, the expression of β-catenin, cyclin D1, MMP7, and c-MYC, key molecules of the Wnt/β-catenin pathway, were decreased or increased by up- or down-regulation of RBM10. We also detected that LUAD cell invasion and migration induced by RBM10 overexpression or silencing were reversed by either CHIR-99021 or XAV-939. To the best of our knowledge, this is the first study that reported how RBM10 inhibits the EMT process of lung adenocarcinoma by regulating the Wnt/β-catenin signaling pathway. Recently, the Wnt/β-catenin signaling pathway has been gradually recognized as a potentially important target for anticancer therapy [27, 50]. Preclinical and clinical studies have shown that inhibitors targeting the Wnt/β-catenin pathway, such as Wnt974, LGX818, OMP-18R5 (Vantictumab), OMP-54F28 (ipafricept), and CWP232291, can successfully inhibit tumors progression. Hence, our results may help improve treatment strategies for

the selection of LUAD patients who may particularly benefit from agents that selectively target blocking the Wnt/β-catenin pathway.

Our results revealed that RBM10 interacts with CTNNBIP1 and positively regulates its expression in LUAD. Previous studies reported that the CTNNBIP1 gene is an antagonist of Wnt signaling [51]. By interacting with β-catenin, CTNNBIP1 disrupts the binding of β-catenin with TCF/LEF complex and down-regulates the expression of downstream target genes of the Wnt signaling pathway (such as c-MYC, CyclinD1, MMP7, etc.), and prevents Wnt/β-catenin signaling pathway activation from inhibiting the progression of LUAD [52, 53]. This finding may explain why TCF3, TCF4, and LEF1 protein levels were reduced by RBM10 in the present study. In our study, down-regulation of CTTNBIP1 expression reversed the cell migration and invasion ability inhibited by overexpression of RBM10 in LUAD cells. Furthermore, we also found that overexpression of RBM10 promoted the inhibitory role of CTNNBIP1, reduced the interaction between β-catenin and TCF/LEF complex while promoting the interaction between β-catenin and CTNNBIP1. Above all, these results indicated that RBM10 abolished the binding of β-catenin and TCF/LEF complex and finally inhibited Wnt/β-catenin signaling to prevent LUAD progression by interacting with CTNNBIP1 and regulating its expression. Whether RBM10 has a direct interaction with CTNNBIP1 and which domain or sequence participates in the above interaction needs to be further studied.

Conclusions

The present study revealed a first working model for how RBM10 inhibits LUAD tumor growth and metastasis (Fig. 8i), indicating that RBM10 may be a potential biomarker and therapeutic target for lung adenocarcinoma. Specifically, RBM10 interacts with CTNBBIP1 and downregulates CTNNBIP1 expression, thereby disrupting the interaction between β-catenin and TCF/LEF complex and inactivating the Wnt/β-catenin pathway. This finding may broaden the understanding of mechanisms involved in LUAD progression; moreover, as a prognostic predictor, RBM10 might be a potential target for LUAD therapy.

Abbreviations

ATCC: American Type Culture Collection

CCK8: cell counting kit-8

Co-IP: Co-immunoprecipitation

CTNNIBIP1: β-catenin interacting protein 1

DMEM: Dulbecco's Modified Eagle's Medium

EdU: Ethynyldeoxyuridine

EMT: Epithelial-mesenchymal transition

FBS: Fetal bovine serum

HE: Hematoxylin-eosin staining

IHC: Immunohistochemical staining

IF: Immunofluorescence

LUAD: lung adenocarcinoma

OS: overall survival

qRT-PCR: quantitation real-time polymerase chain reaction

RBM10: RNA-binding motif protein 10

RBP: RNA-binding protein

Declarations

Ethics approval and consent to participate

This research protocol was approved by the Third Clinical Ethics Committee of Harbin Medical University and a consent form was signed by each participating patient.

Consent for publication

Not applicable.

Availability of data and materials

The authors state that all data supporting the findings of this study are available in this study and its supplementary information files, or by reasonable request of the corresponding authors.

Competing interests

The authors declare that they have no conflict of interest.

Founding

This work was supported by Post graduate research and practice innovation project of Harbin Medical University (YJSKYCX2019-58HYD), the National Natural Science Foundation of China (81872396 and

81672931), the National Cancer Center of China Climbing Fund (NCC201808B017), and Hei Long Jiang Postdoctoral Foundation (LBH-Z18196).

Author contributions

YYC, BP and YY designed research; YYC performed the experiments and drafted the manuscript; XW contributed to qRT-PCR assay; JXG and SQX was involved in the western blot assay; YGL collected the human LUAD fresh tissues; YXZ and ZXW performed the immunofluorescent staining; YYC, LSQ and ZJW analyzed data; QWM and YY managed the experimental design, reviewed the manuscript. All authors read and approved the final manuscript.

Acknowledgements

We owe our thanks to all lab personnel in this study.

References

1. Lambe G, Durand M, Buckley A, Nicholson S, McDermott R: Adenocarcinoma of the lung: from BAC to the future. *Insights into imaging* 2020, 11:69.
2. Sung H, Ferlay J, Siegel RL, Laversanne M, Soerjomataram I, Jemal A, Bray F: Global cancer statistics 2020: GLOBOCAN estimates of incidence and mortality worldwide for 36 cancers in 185 countries. *CA: a cancer journal for clinicians* 2021.
3. Lee JJ, Park S, Park H, Kim S, Lee J, Lee J, Youk J, Yi K, An Y, Park IK, et al: Tracing Oncogene Rearrangements in the Mutational History of Lung Adenocarcinoma. *Cell* 2019, 177:1842-1857 e1821.
4. Paez JG, Janne PA, Lee JC, Tracy S, Greulich H, Gabriel S, Herman P, Kaye FJ, Lindeman N, Boggon TJ, et al: EGFR mutations in lung cancer: correlation with clinical response to gefitinib therapy. *Science* 2004, 304:1497-1500.
5. Kwak EL, Bang YJ, Camidge DR, Shaw AT, Solomon B, Maki RG, Ou SH, Dezube BJ, Janne PA, Costa DB, et al: Anaplastic lymphoma kinase inhibition in non-small-cell lung cancer. *The New England journal of medicine* 2010, 363:1693-1703.
6. Bergethon K, Shaw AT, Ou SH, Katayama R, Lovly CM, McDonald NT, Massion PP, Siwak-Tapp C, Gonzalez A, Fang R, et al: ROS1 rearrangements define a unique molecular class of lung cancers. *Journal of clinical oncology : official journal of the American Society of Clinical Oncology* 2012, 30:863-870.
7. Hill A, Fisher P, Yeomanson D: Non-small cell lung cancer. *Bmj* 2012, 345:e6443.

8. Chen H, Carrot-Zhang J, Zhao Y, Hu H, Freeman SS, Yu S, Ha G, Taylor AM, Berger AC, Westlake L, et al: Genomic and immune profiling of pre-invasive lung adenocarcinoma. *Nature communications* 2019, 10:5472.
9. Imielinski M, Berger AH, Hammerman PS, Hernandez B, Pugh TJ, Hodis E, Cho J, Suh J, Capelletti M, Sivachenko A, et al: Mapping the hallmarks of lung adenocarcinoma with massively parallel sequencing. *Cell* 2012, 150:1107-1120.
10. Sebestyen E, Singh B, Minana B, Pages A, Mateo F, Pujana MA, Valcarcel J, Eyras E: Large-scale analysis of genome and transcriptome alterations in multiple tumors unveils novel cancer-relevant splicing networks. *Genome Res* 2016, 26:732-744.
11. Giannakis M, Mu XJ, Shukla SA, Qian ZR, Cohen O, Nishihara R, Bahl S, Cao Y, Amin-Mansour A, Yamauchi M, et al: Genomic Correlates of Immune-Cell Infiltrates in Colorectal Carcinoma. *Cell reports* 2016, 15:857-865.
12. Vinayanuwattikun C, Le Calvez-Kelm F, Abedi-Ardekani B, Zaridze D, Mukeria A, Voegele C, Vallee M, Purnomosari D, Forey N, Durand G, et al: Elucidating Genomic Characteristics of Lung Cancer Progression from In Situ to Invasive Adenocarcinoma. *Scientific reports* 2016, 6:31628.
13. Loiselle JJ, Sutherland LC: RBM10: Harmful or helpful-many factors to consider. *Journal of cellular biochemistry* 2018, 119:3809-3818.
14. Bechara EG, Sebestyen E, Bernardis I, Eyras E, Valcarcel J: RBM5, 6, and 10 differentially regulate NUMB alternative splicing to control cancer cell proliferation. *Molecular cell* 2013, 52:720-733.
15. Mueller CF, Berger A, Zimmer S, Tiyerili V, Nickenig G: The heterogenous nuclear riboprotein S1-1 regulates AT1 receptor gene expression via transcriptional and posttranscriptional mechanisms. *Archives of biochemistry and biophysics* 2009, 488:76-82.
16. Han LP, Wang CP, Han SL: Overexpression of RBM10 induces osteosarcoma cell apoptosis and inhibits cell proliferation and migration. *Medecine sciences : M/S* 2018, 34 Focus issue F1:81-86.
17. Martinez-Arribas F, Agudo D, Pollan M, Gomez-Esquer F, Diaz-Gil G, Lucas R, Schneider J: Positive correlation between the expression of X-chromosome RBM genes (RBMX, RBM3, RBM10) and the proapoptotic Bax gene in human breast cancer. *Journal of cellular biochemistry* 2006, 97:1275-1282.
18. Loiselle JJ, Roy JG, Sutherland LC: RBM10 promotes transformation-associated processes in small cell lung cancer and is directly regulated by RBM5. *PloS one* 2017, 12:e0180258.
19. Sun X, Jia M, Sun W, Feng L, Gu C, Wu T: Functional role of RBM10 in lung adenocarcinoma proliferation. *International journal of oncology* 2019, 54:467-478.
20. Witkiewicz AK, McMillan EA, Balaji U, Baek G, Lin WC, Mansour J, Mollaee M, Wagner KU, Koduru P, Yopp A, et al: Whole-exome sequencing of pancreatic cancer defines genetic diversity and therapeutic targets. *Nature communications* 2015, 6:6744.
21. Garrisi VM, Strippoli S, De Summa S, Pinto R, Perrone A, Guida G, Azzariti A, Guida M, Tommasi S: Proteomic profile and in silico analysis in metastatic melanoma with and without BRAF mutation. *PloS one* 2014, 9:e112025.

22. Zhou P, Li Y, Li B, Zhang M, Liu Y, Yao Y, Li D: NMIIA promotes tumor growth and metastasis by activating the Wnt/beta-catenin signaling pathway and EMT in pancreatic cancer. *Oncogene* 2019, 38:5500-5515.
23. Zhang H, Wu X, Xiao Y, Wu L, Peng Y, Tang W, Liu G, Sun Y, Wang J, Zhu H, et al: Coexpression of FOXK1 and vimentin promotes EMT, migration, and invasion in gastric cancer cells. *J Mol Med (Berl)* 2019, 97:163-176.
24. Kalluri R, Weinberg RA: The basics of epithelial-mesenchymal transition. *The Journal of clinical investigation* 2009, 119:1420-1428.
25. Rapp J, Jaromi L, Kvell K, Miskei G, Pongracz JE: WNT signaling - lung cancer is no exception. *Respiratory research* 2017, 18:167.
26. Chen J, Hu L, Chen J, Pan Q, Ding H, Xu G, Zhu P, Wen X, Huang K, Wang Y: Detection and Analysis of Wnt Pathway Related lncRNAs Expression Profile in Lung Adenocarcinoma. *Pathology oncology research : POR* 2016, 22:609-615.
27. Stewart DJ: Wnt signaling pathway in non-small cell lung cancer. *Journal of the National Cancer Institute* 2014, 106:djt356.
28. Qi J, Yu Y, Akilli Ozturk O, Holland JD, Besser D, Fritzmann J, Wulf-Goldenberg A, Eckert K, Fichtner I, Birchmeier W: New Wnt/beta-catenin target genes promote experimental metastasis and migration of colorectal cancer cells through different signals. *Gut* 2016, 65:1690-1701.
29. Yang S, Liu Y, Li MY, Ng CSH, Yang SL, Wang S, Zou C, Dong Y, Du J, Long X, et al: FOXP3 promotes tumor growth and metastasis by activating Wnt/beta-catenin signaling pathway and EMT in non-small cell lung cancer. *Mol Cancer* 2017, 16:124.
30. Mao J, Fan S, Ma W, Fan P, Wang B, Zhang J, Wang H, Tang B, Zhang Q, Yu X, et al: Roles of Wnt/beta-catenin signaling in the gastric cancer stem cells proliferation and salinomycin treatment. *Cell death & disease* 2014, 5:e1039.
31. Reifenberger J, Knobbe CB, Wolter M, Blaschke B, Schulte KW, Pietsch T, Ruzicka T, Reifenberger G: Molecular genetic analysis of malignant melanomas for aberrations of the WNT signaling pathway genes CTNNB1, APC, ICAT and BTRC. *International journal of cancer* 2002, 100:549-556.
32. Guo M, Zhang X, Wang G, Sun J, Jiang Z, Khadarian K, Yu S, Zhao Y, Xie C, Zhang K, et al: miR-603 promotes glioma cell growth via Wnt/beta-catenin pathway by inhibiting WIF1 and CTNNBIP1. *Cancer letters* 2015, 360:76-86.
33. Koyama T, Tago K, Nakamura T, Ohwada S, Morishita Y, Yokota J, Akiyama T: Mutation and expression of the beta-catenin-interacting protein ICAT in human colorectal tumors. *Japanese journal of clinical oncology* 2002, 32:358-362.
34. Jiang Y, Ren W, Wang W, Xia J, Gou L, Liu M, Wan Q, Zhou L, Weng Y, He T, Zhang Y: Inhibitor of beta-catenin and TCF (ICAT) promotes cervical cancer growth and metastasis by disrupting E-cadherin/beta-catenin complex. *Oncology reports* 2017, 38:2597-2606.
35. Chang JM, Tsai AC, Huang WR, Tseng RC: The Alteration of CTNNBIP1 in Lung Cancer. *International journal of molecular sciences* 2019, 20.

36. Zhou F, Geng J, Xu S, Meng Q, Chen K, Liu F, Yang F, Pan B, Yu Y: FAM83A signaling induces epithelial-mesenchymal transition by the PI3K/AKT/Snail pathway in NSCLC. *Aging* 2019, 11:6069-6088.
37. Sun BO, Fang Y, Li Z, Chen Z, Xiang J: Role of cellular cytoskeleton in epithelial-mesenchymal transition process during cancer progression. *Biomedical reports* 2015, 3:603-610.
38. Veeman MT, Axelrod JD, Moon RT: A second canon. Functions and mechanisms of beta-catenin-independent Wnt signaling. *Developmental cell* 2003, 5:367-377.
39. Cadigan KM, Waterman ML: TCF/LEFs and Wnt signaling in the nucleus. *Cold Spring Harbor perspectives in biology* 2012, 4.
40. Liu CC, Cai DL, Sun F, Wu ZH, Yue B, Zhao SL, Wu XS, Zhang M, Zhu XW, Peng ZH, Yan DW: FERMT1 mediates epithelial-mesenchymal transition to promote colon cancer metastasis via modulation of beta-catenin transcriptional activity. *Oncogene* 2017, 36:1779-1792.
41. Li H, Zhang W, Yan M, Qiu J, Chen J, Sun X, Chen X, Song L, Zhang Y: Nucleolar and spindle associated protein 1 promotes metastasis of cervical carcinoma cells by activating Wnt/beta-catenin signaling. *J Exp Clin Cancer Res* 2019, 38:33.
42. Vogelstein B, Papadopoulos N, Velculescu VE, Zhou S, Diaz LA, Jr., Kinzler KW: Cancer genome landscapes. *Science* 2013, 339:1546-1558.
43. Rodor J, FitzPatrick DR, Eyras E, Caceres JF: The RNA-binding landscape of RBM10 and its role in alternative splicing regulation in models of mouse early development. *RNA biology* 2017, 14:45-57.
44. Nusse R, Clevers H: Wnt/beta-Catenin Signaling, Disease, and Emerging Therapeutic Modalities. *Cell* 2017, 169:985-999.
45. Akiri G, Cherian MM, Vijayakumar S, Liu G, Bafico A, Aaronson SA: Wnt pathway aberrations including autocrine Wnt activation occur at high frequency in human non-small-cell lung carcinoma. *Oncogene* 2009, 28:2163-2172.
46. Scherly D, Boelens W, Dathan NA, van Venrooij WJ, Mattaj IW: Major determinants of the specificity of interaction between small nuclear ribonucleoproteins U1A and U2B" and their cognate RNAs. *Nature* 1990, 345:502-506.
47. Query CC, Bentley RC, Keene JD: A common RNA recognition motif identified within a defined U1 RNA binding domain of the 70K U1 snRNP protein. *Cell* 1989, 57:89-101.
48. Hao YQ, Su ZZ, Lv XJ, Li P, Gao P, Wang C, Bai Y, Zhang J: RNA-binding motif protein 5 negatively regulates the activity of Wnt/beta-catenin signaling in cigarette smoke-induced alveolar epithelial injury. *Oncology reports* 2015, 33:2438-2444.
49. Jiang Y, Sheng H, Meng L, Yue H, Li B, Zhang A, Dong Y, Liu Y: RBM5 inhibits tumorigenesis of gliomas through inhibition of Wnt/beta-catenin signaling and induction of apoptosis. *World journal of surgical oncology* 2017, 15:9.
50. Krishnamurthy N, Kurzrock R: Targeting the Wnt/beta-catenin pathway in cancer: Update on effectors and inhibitors. *Cancer treatment reviews* 2018, 62:50-60.

51. Kosari-Monfared M, Nikbakhsh N, Fattahi S, Ghadami E, Ranaei M, Taheri H, Amjadi-Moheb F, Godazandeh GA, Shafaei S, Pilehchian-Langroudi M, et al: CTNNBIP1 downregulation is associated with tumor grade and viral infections in gastric adenocarcinoma. *Journal of cellular physiology* 2019, 234:2895-2904.
52. Stow JL: ICAT is a multipotent inhibitor of beta-catenin. Focus on "role for ICAT in beta-catenin-dependent nuclear signaling and cadherin functions". *American journal of physiology Cell physiology* 2004, 286:C745-746.
53. Gooding JM, Yap KL, Ikura M: The cadherin-catenin complex as a focal point of cell adhesion and signalling: new insights from three-dimensional structures. *BioEssays : news and reviews in molecular, cellular and developmental biology* 2004, 26:497-511.

Figures

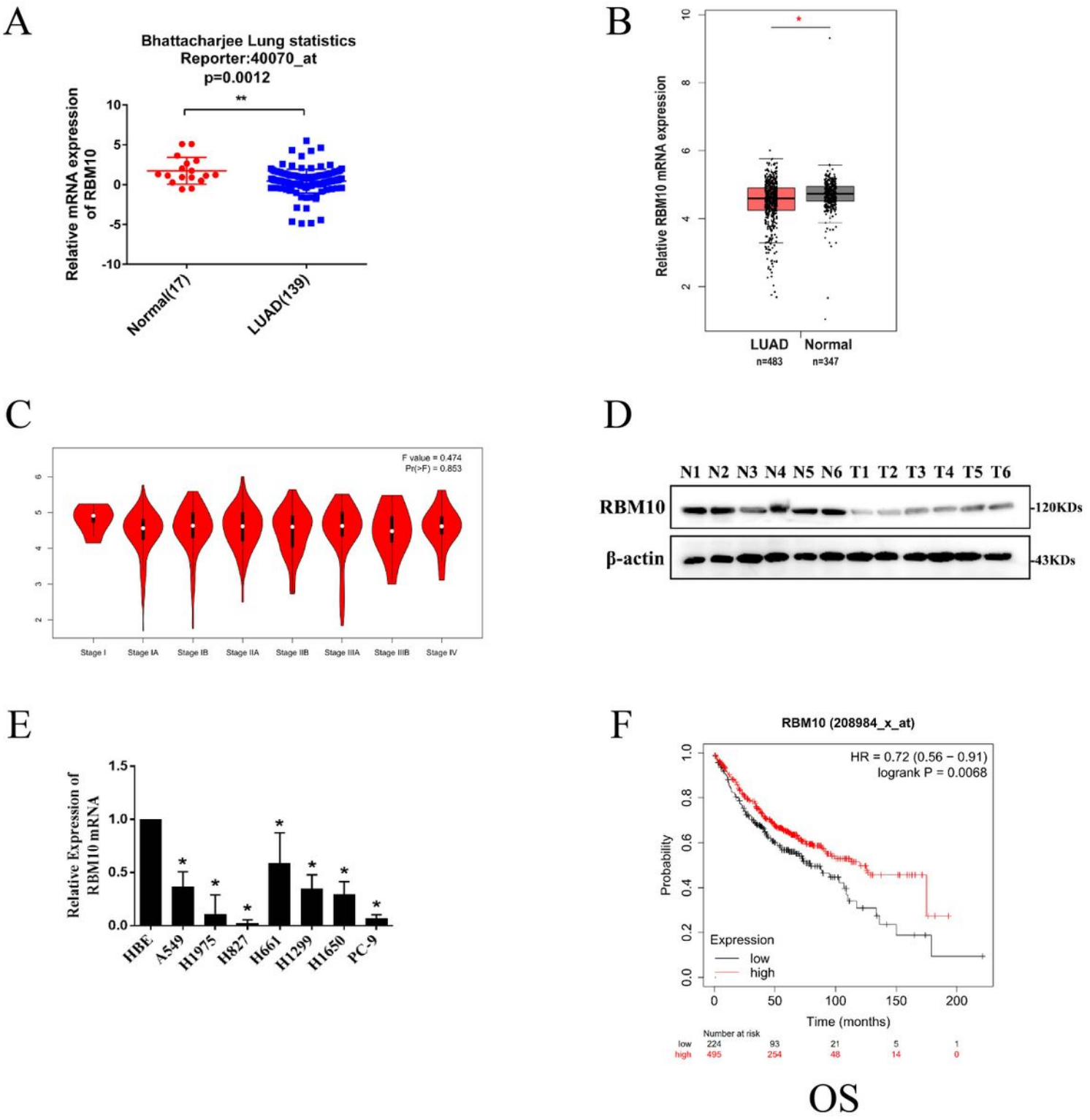

Figure 1

RBM10 expression in LUAD tissues (a) RBM10 mRNA levels of LUAD compared with the normal lung sample in Bhattacharjee lung Oncomine statistics (http://www.oncomine.org). (b) The boxplot analysis showed the RBM10 mRNA expression level in LUAD from TCGA and GTEx database on the GEPIA website (http://gepia.cancer-pku.cn/). (c) The box plots showed that expression levels of RBM10 were gradually decreased with T-stage progression. (d) Western blot analysis of the protein expression of

RBM10 in sex pairs of human LUAD fresh tissues. (e) qRT-PCR results of the mRNA expression of RBM10 in eight LUAD cell lines (H1299, H1915, H1650, A549, H1975, H661, H827, PC-9) and the normal lung epithelial cell line HBE. The results were represented as mean ± SD. *P<0.05. (f) Kaplan-Meier plotter database (http://kmplot.com) was searched for the overall survival of LUAD patients.

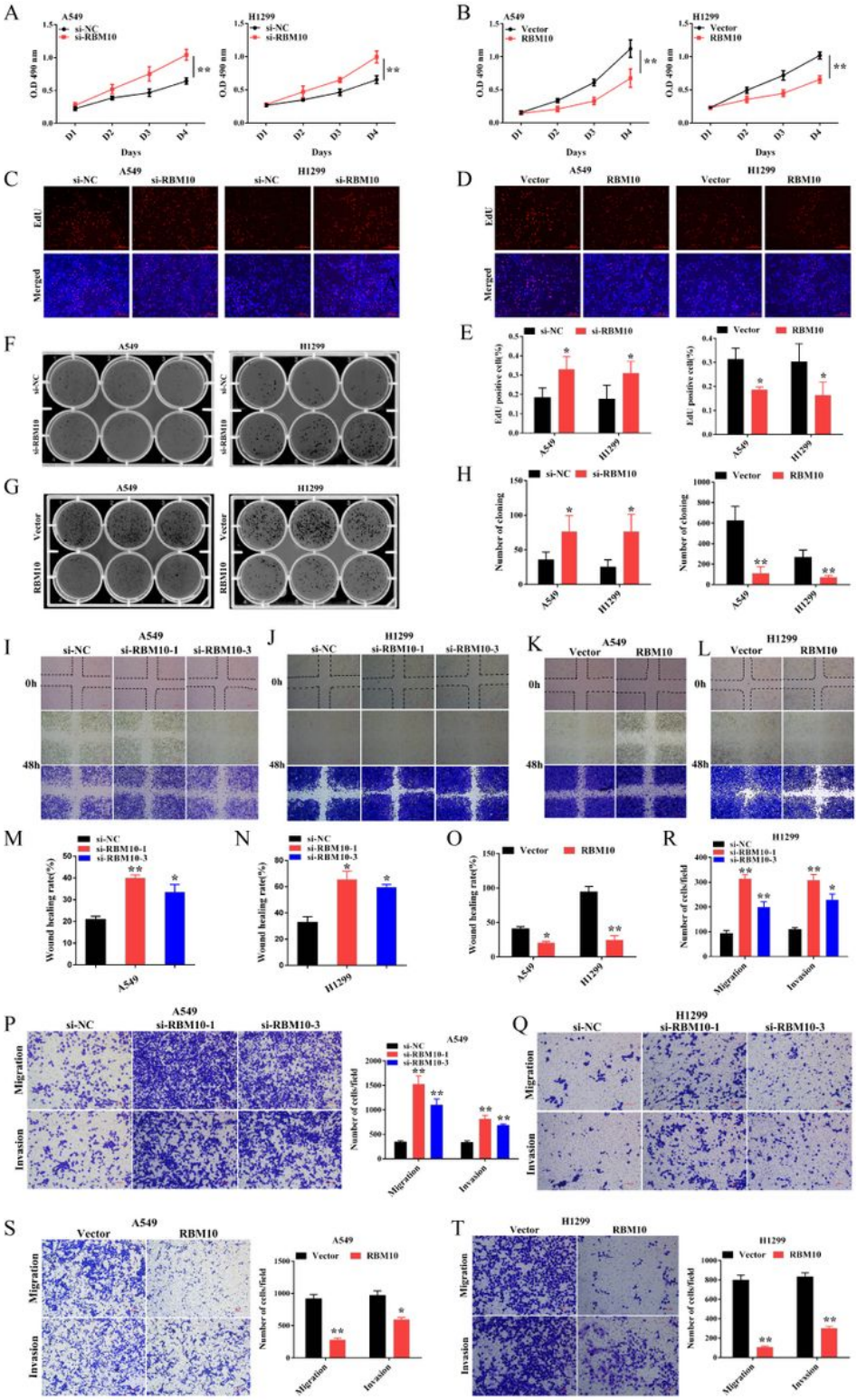

Figure 2

RBM10 decreases cell proliferation, migration, and invasion of LUAD cells in vitro. RBM10 was silenced or overexpressed in A549 and H1299 cell lines. (a, b) Cell proliferation was examined by CCK8; (c ~e) EdU; (g ~h) colony formation assays. The results were represented as mean ± SD, *P < 0.05, **P < 0.01. (i ~o) A wound-healing assay was used to test the migration capacity of RBM10 in LUAD cells. The cells migrating into the wounded areas were photographed at 0h and 48h. The results were represented as mean ± SD, *P < 0.05, **P < 0.01, Scale bar is 100μm. (q ~t) The migration and invasion capacity of RBM10 in LUAD cells were also examined by Transwell assays. The results were represented as mean ± SD, *P < 0.05, **P < 0.01, Scale bar is 100μm. Each experiment was repeated three times.

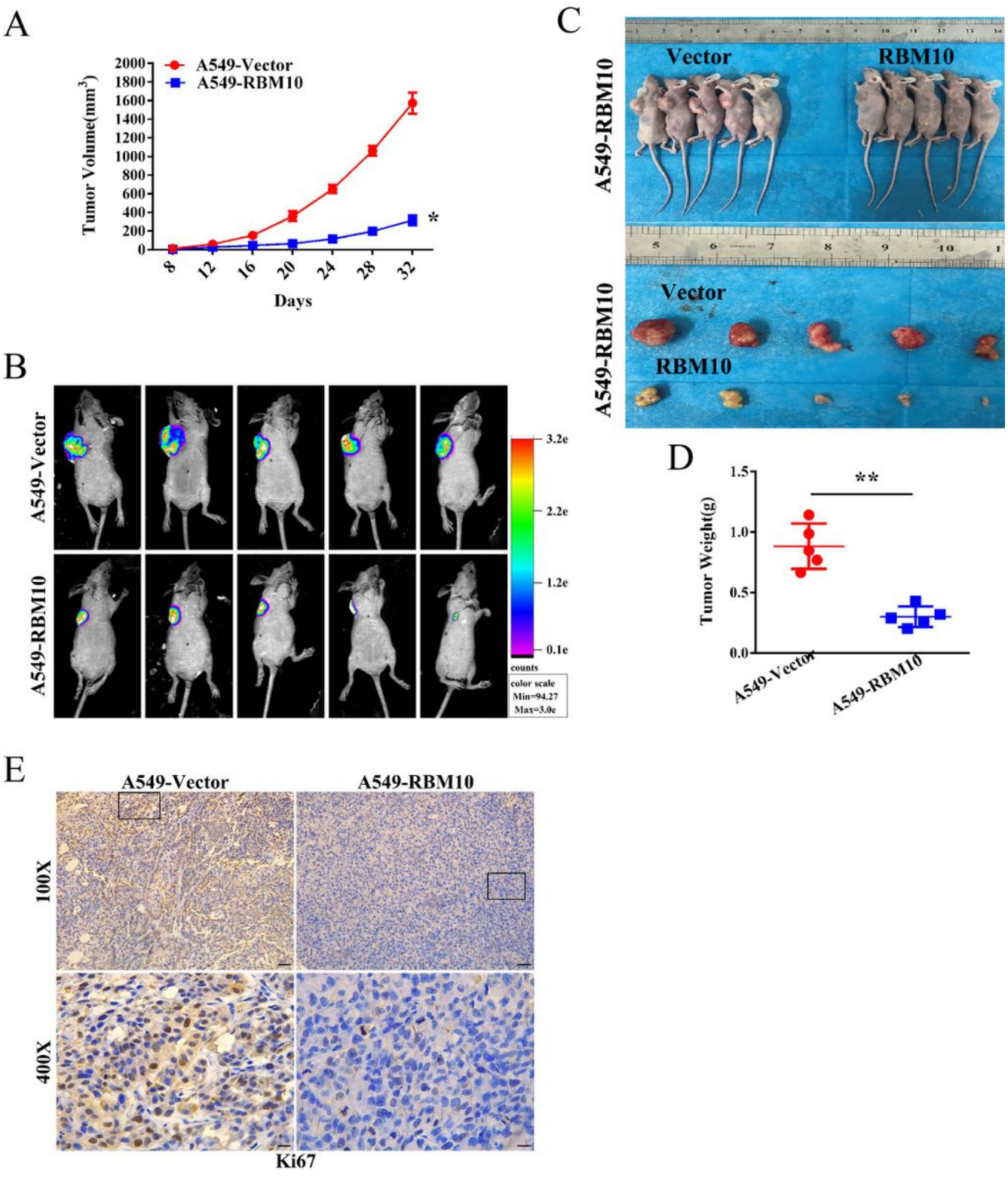

Figure 3

RBM10 overexpression inhibited tumor growth in vivo. Approximately 2.5 × 107/150μl A549 cells expressing RBM10 were injected into the left armpit of 4 weeks BALB/c nude mice (n=5 mice per group); tumor volume was measured after sizeable tumors formation (day 8), and measured every 4 days. On day 32, the inoculated mice were sacrificed, photographed, and the tumor was weighted. (a) The subcutaneous tumor volume curves. (b) Representative images of bioluminescence imaging (BLI) of the

nude mice 32 days after injection of indicated cells. (c) Representative gross photos of mice and the tumor lumps from the indicated groups at the endpoint of the experiment. (d) Tumor weight was measured. (e) The expression of ki67 in tumor tissues was determined by IHC. The results were represented as mean ± SD, *p<0.05, **p<0.01

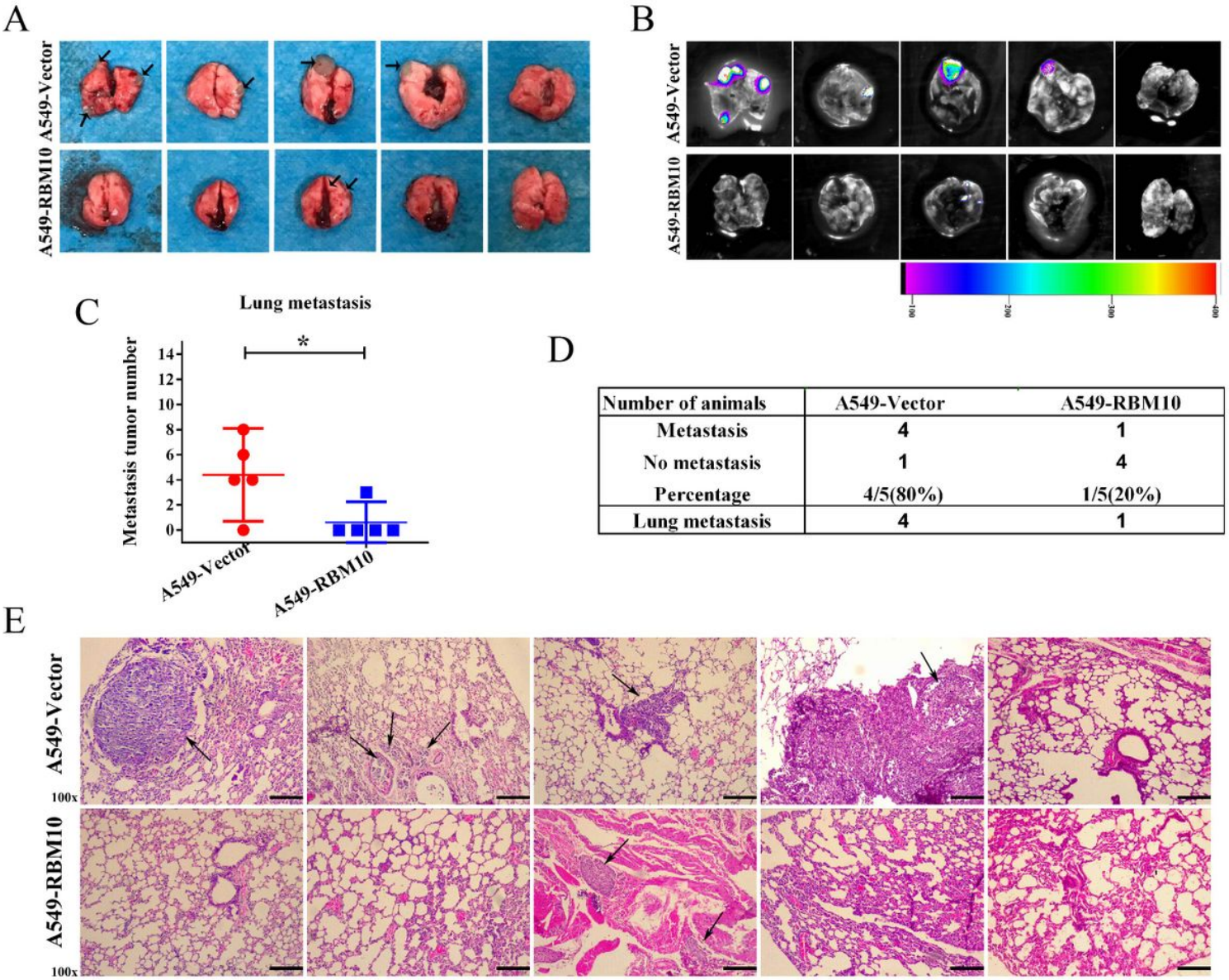

Number of animals	A549-Vector	A549-RBM10
Metastasis	4	1
No metastasis	1	4
Percentage	4/5(80%)	1/5(20%)
Lung metastasis	4	1

Figure 4

RBM10 overexpression inhibited lung metastasis in vivo. A total of 1 × 107/150μl stable RBM10 overexpression A549 cells were injected in nude mice through the tail vein to establish lung metastasis models (n=5 mice per group). (a, b) After week 7, after tail vein injection, the lungs of mice were removed. (a) Representative gross images of the lungs from different experimental groups. (b) typical bioluminescence images of lung metastases; arrows indicate metastatic surface nodules. (c) Box-scatter plot shows the number of metastatic nodules in the lung as observed in each group. The results were represented as mean ± SD, *p<0.05. (d) Statistical analysis of lung metastasis in the two groups of nude

mice. (e) Typical H&E staining pictures of lung metastasis lesions were shown. Arrows indicate metastatic surface nodules.

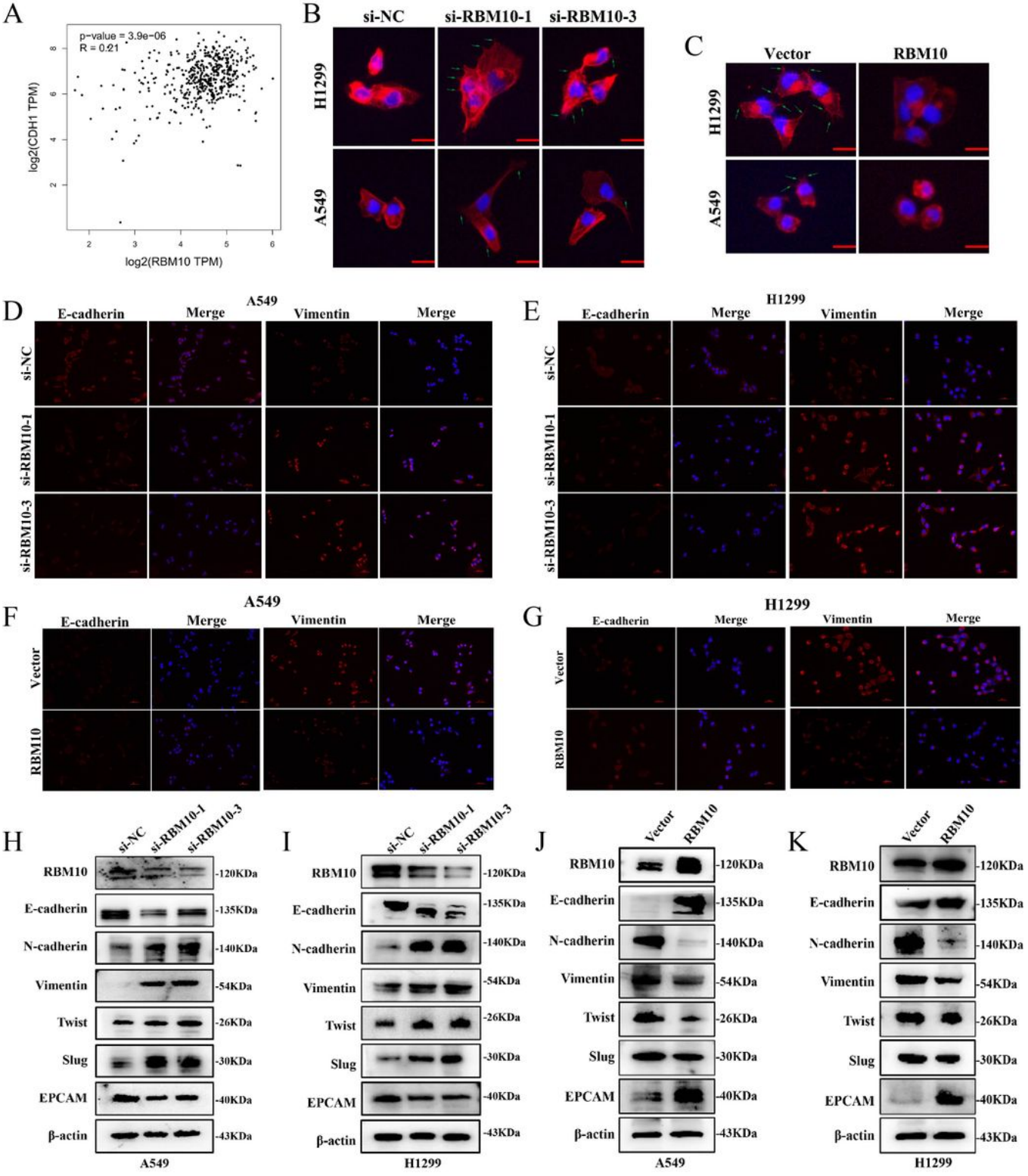

Figure 5

RBM10 inhibited EMT in LUAD cells. (a) Positive correlation between RBM10 and CDH1(E-cadherin) in LUAD, analyzed at the GEPIA website. (b, c) Rearrangements of the cytoskeleton in A549 and H1299 cells when RBM10 was up- or down-regulated. (d ~g) Immunofluorescence analysis used to observe the

expression of epithelial cell markers E-cadherin (red) and mesenchymal cell markers vimentin (red) in A549 and NCI-H1299 cells with knockdown (d, e) or over-expressing (f, g) RBM10. Nuclei counterstained with DAPI (blue). (h ~k) Western blot analysis of the EMT markers (E-cadherin, Vimentin, slug, twist, N-cadherin) and adhesion molecule EPCAM in A549 or NCI-H1299 cells with knockdown (h, i) or overexpressing (j, k) RBM10.

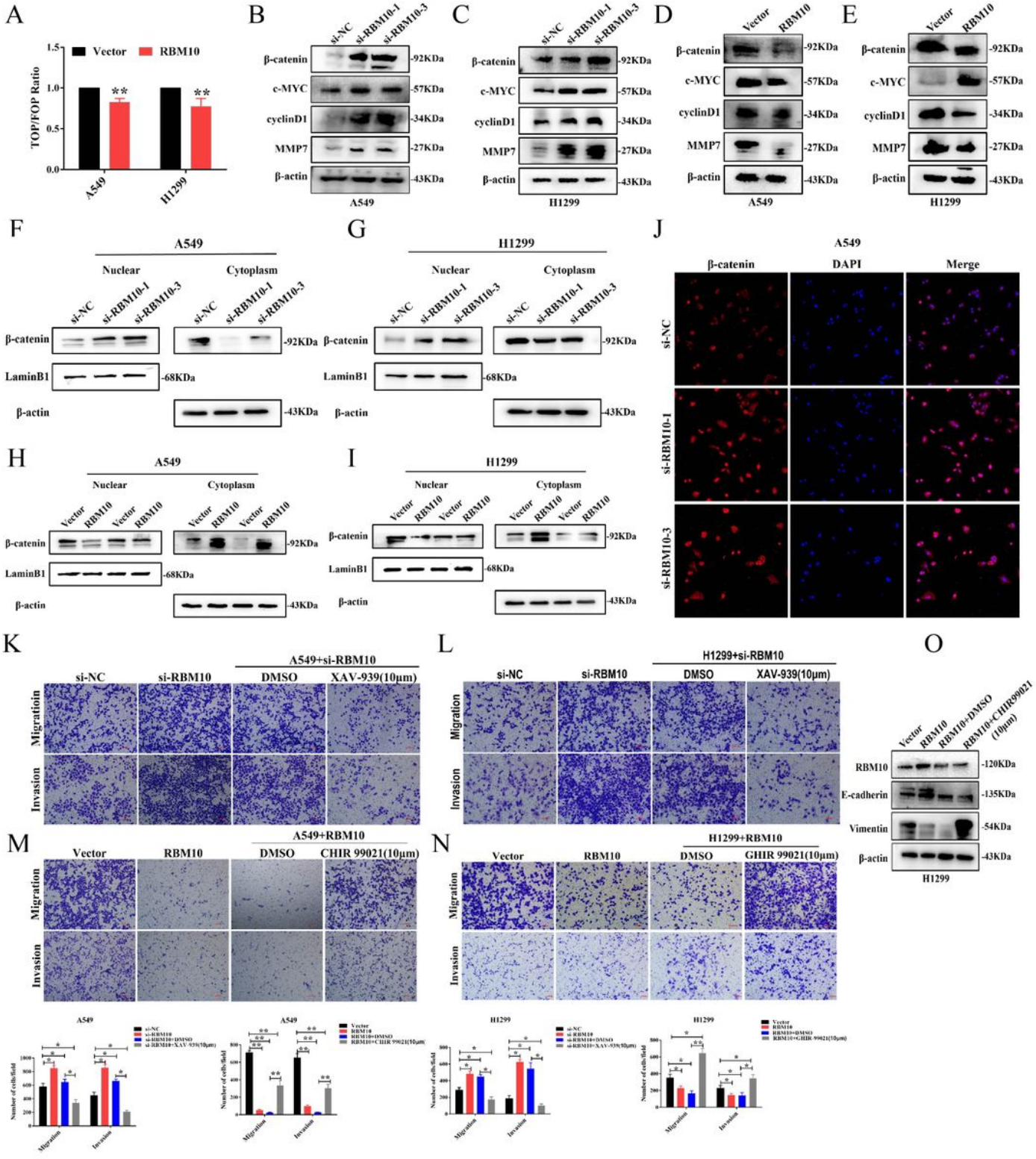

Figure 6

RBM10 inactivated Wnt/β-catenin pathway in LUAD cells. (a) The TOP/FOP reporter assay was used to examine the activity of the Wnt/β-catenin pathway in RBM10-overexpressing A549 and H1299 cells. (b ~e) β-catenin, cyclinD1, c-MYC, and MMP7 levels were detected by Western blot in LUAD cells with RBM10 knockdown (b, c) or overexpression (d, e) respectively. (f ~i) Western blot assay nuclear and cytoplasmic cellular fractions utilized to detect the nuclear translocation of β-catenin. β-actin was the cytoplasmic control, and LaminB1 was the nuclear control. (j) Subcellular localization of β-catenin in RBM10-silencing A549 cells was detected by immunofluorescence assay. (k, l) A Wnt/β-catenin pathway inhibitor, XAV-939 (10μM), was used to treat the RBM10-silencing cells and the control cells for 48 h. The invasive and migration abilities of A549 and H1299 cells were tested by Transwell assay. (m, n) A Wnt/β-catenin pathway activator, CHIR 99021 (10μM), was used to treat the RBM10-overexpressing cells and the control cells for 48 h. The invasive and migration abilities of LUAD cells (A549 and H1299) were evaluated by Transwell assay. (o) The protein levels of E-cadherin, a twist of H1299-RBM10 cells treated with CHIR 99021 (10μM) was determined using western blot. The results were represented as mean ± SD. *$p<0.05$, **$p<0.01$. All experiments were repeated three times.

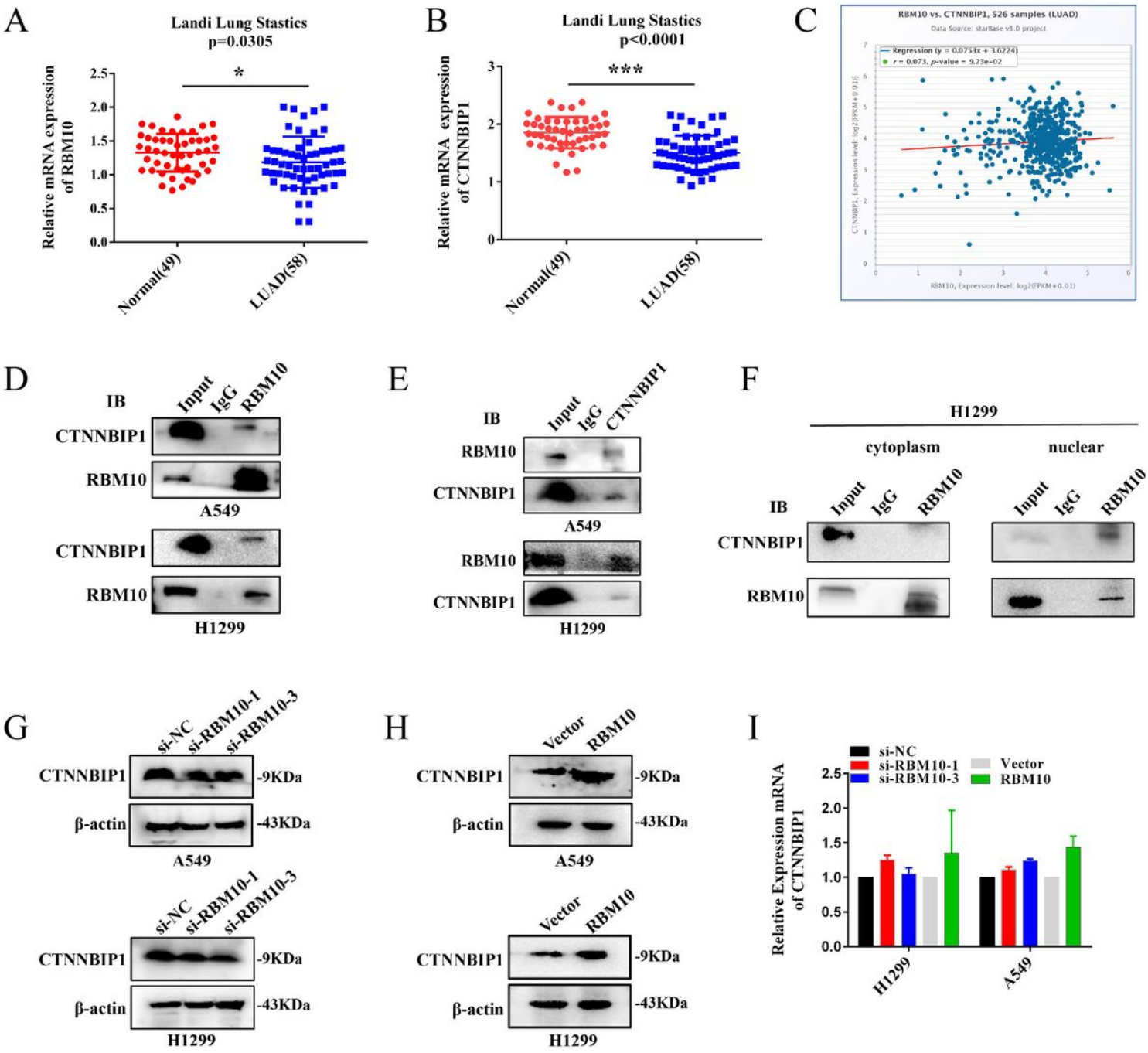

Figure 7

RBM10 interacts with CTNNBIP1. (a, b) The mRNA expression of RBM10 (a) and CTNNBIP1 (b) were analyzed based on the Landi lung cohort in Oncomine starbase. (c) A positive correlation between RBM10 mRNA and CTNNBIP1 mRNA was found in the LUAD-TCGA cohort from StarBase (c) databases. (d, e) Co-immunoprecipitation (Co-IP) was used to validate the interaction of RBM10 and CTNNBIP1. (d) RBM10 was pulled down by anti-RBM10, and Western blot was used to detect RBM10 and CTNNBIP1. (e) CTNNBIP1 was pulled down by anti-CTNNBIP1, and then RBM10 and CTNNBIP1 were detected by western blot. (f) co-IP assay of the nuclear and cytoplasmic cellular fractions revealed that RBM10 mainly interacted with CTNNBIP1 in the nucleus. (g, h) Western blot assay was utilized to detect RBM10 and CTNNBIP1 expressions in RBM10 knockdown (g) or overexpression (h) cells. β-actin was used as

loading controls. (i) qTR-PCR result of RBM10 and CTNNBIP1 mRNA expressions under RBM10 knockdown or overexpression. Both down-regulation or upregulation of RBM10 did not alter CTNNBIP1 mRNA. GAPDH was used as loading controls. The results were represented as mean ± SD. *P < 0.05, All experiments were repeated three times.

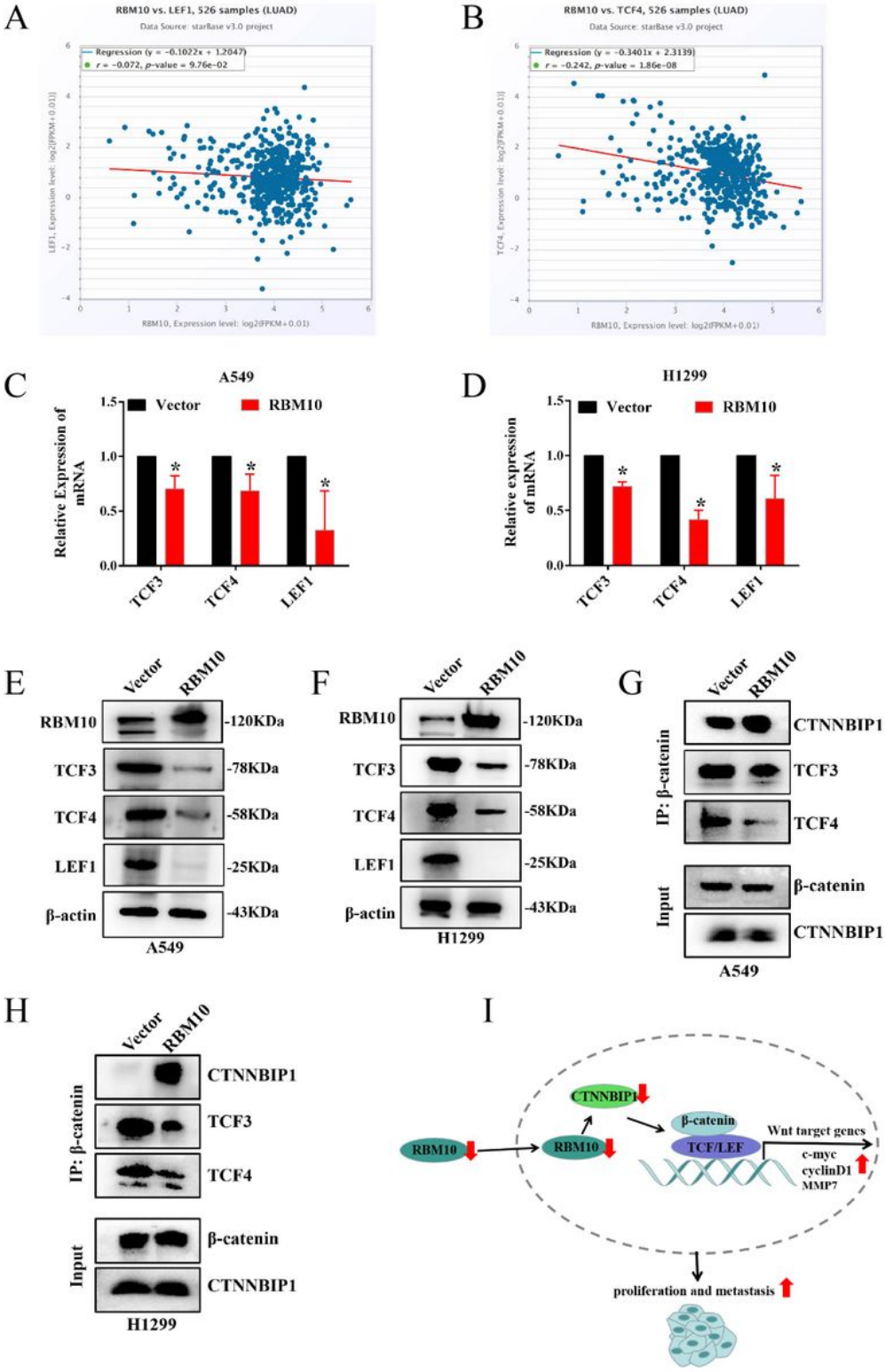

Figure 8

RBM10 inhibits the Wnt/β-catenin pathway by blocking the β-catenin-TCF/LEF interaction. (a, b) Studies from StarBase datasets showed that RBM10 expression was negatively corrected with the expression of LEF1 (a) and TCF4 (b) in LUAD samples. (c, d) qRT-PCR results of TCF3, TCF4, LEF1 mRNA levels under RBM10 overexpression, GAPDH was used as loading controls. (e, f) Western blot data of TCF3, TCF4, LEF1 protein levels under RBM10 overexpression, β-actin was used as loading controls. (g, h) Co-IP was used to test β-catenin interaction analyses using a β-catenin antibody. Western blot showed that upregulation of RBM10 decreased β-catenin-TCF/LEF interaction, whereas promoting CTNNBIP1/β-catenin interaction. (i) A schematic diagram of the functional roles of RBM10 in LUAD cells. The results were represented as mean ± SD. All *P < 0.05 All experiments were repeated three times.

Supplementary Files

This is a list of supplementary files associated with this preprint. Click to download.

- supplementaryinformation.docx